Extracting nondispersive charge carrier mobilities of organic semiconductors from simulations of small systems

Alexander Lukyanov* and Denis Andrienko†
Max Planck Institute for Polymer Research, Ackermannweg 10, 55128 Mainz, Germany
(Received 26 August 2010; revised manuscript received 6 October 2010; published 9 November 2010)

Predictions of charge-carrier mobilities in amorphous semiconductors often rely on charge transport simulations in microscopically sized systems, where transport is dispersive and mobilities are system-size dependent. We propose a method for extrapolating a macroscopic nondispersive mobility from the temperature dependence of a microscopic one. The method is tested on an amorphous phase of tris(8-hydroxyquinoline) aluminum, for which the temperature dependence of a microscopic hole mobility is obtained by combining molecular-dynamics simulations for generating material morphologies, electronic-structure calculations for determining charge hopping rates, and kinetic Monte Carlo simulations for studying charge dynamics. The extracted value of the nondispersive mobility and its electric field dependence agree well with the results of time-of-flight experiments.

DOI: 10.1103/PhysRevB.82.193202 PACS number(s): 72.80.Le, 71.23.−k, 72.80.Ph, 73.63.Bd

Organic semiconductors define an important class of cost-effective, lightweight, and mechanically flexible materials which are being employed in organic light-emitting diodes, field-effect transistors, and solar cells. While the advantage of organic materials is their synthetically tunable electronic and self-assembling properties, such a vast amount of compounds requires prescreening or, in other words, formulation of structure-processing-property relationships needed for rational compound design.[1,2] Special attention should be paid to parameter-free predictions of charge carrier mobilities, which are important for short circuit currents in solar cells, on/off ratios in field-effect transistors, and a balanced hole/electron transport in light-emitting diodes.

In spite of their technological importance, predictions of charge-carrier dynamics in such materials are extremely difficult to make. First, dynamics of nuclei and electrons may take place over the same time scale, making it impossible to separate nuclear and electronic degrees of freedom.[3] Second, charge transport in organic semiconductors is a truly multiscale problem, as charge-carrier mobility is a function of molecular electronic structure,[4] local molecular orientations and positions,[5] as well as the global topology of a charge percolating network.[6]

Addressing the first problem, the nuclear dynamics is much slower than the dynamics of charge carriers in the majority of disordered organic semiconductors. Hence, the latter can be described by a Hamiltonian with static disorder based on the electronic density of localized states and the hopping rates between them.[7,8] This separation of fast and slow degrees of freedom is typical for the amorphous materials considered in this study.

The second problem can be tackled by explicitly simulating the materials morphology using molecular dynamics. This morphology may then be used to compute charge-transfer rates, ω_{ij}, between the molecules i and j by applying Marcus theory,[9]

$$\omega_{ij} = \frac{J_{ij}^2}{\hbar}\sqrt{\frac{\pi}{\lambda k_B T}}\exp\left[-\frac{(\Delta G_{ij}-\lambda)^2}{4\lambda k_B T}\right], \quad (1)$$

where J_{ij} is the intermolecular transfer integral, λ is the reorganization energy, and $\Delta G_{ij}=\epsilon_j-\epsilon_i$ is the free-energy difference between the initial and final states. Charge-carrier mobility is then obtained either by using kinetic Monte Carlo (KMC) simulations or by solving master equations. This approach relates charge transport properties directly to the chemical structure and has been used in the past to calculate mobility in columnar discotic mesophases,[1,5,10–12] amorphous systems,[13–15] self-assembled monolayers,[6] and conjugated polymers.[16,17]

The bottleneck of this approach is the computationally demanding evaluation of hopping rates for each pair of neighboring molecules, in particular, intermolecular transfer integrals.[18] If density-functional theory is employed, systems of up to several thousand molecules can be treated.[19] As a result, simulated systems are normally only several nanometer thick and, if energetic disorder is present, i.e., site-to-site variations in ϵ_i, charge transport is very likely to be dispersive at room temperature.[20,21] Hence, measured mobility will be system-size dependent since a charge carrier injected at a certain energy level will not visit enough sites to reach an equilibrium state before it is collected. Thus, dispersive transport occurs in all amorphous organic materials for small system sizes and low temperatures.[21]

In simulations, the box is often duplicated in the direction of the field before charge dynamics is studied. This seemingly straightforward increase in the system size will indeed result in nondispersive transients but is still incorrect since all periodically duplicated boxes have exactly the same (small) number of site energies, defining the equilibrium energy of a charge. Hence, charge carriers would traverse the sample at a different (higher) temperature than in an infinitely large system. On the other hand, in time-of-flight (TOF) experiments, a typical sample thickness is in the micrometer range and transport is often nondispersive. To link simulation and experiment, one needs to extract the nondispersive mobility from simulations of small systems, where charge transport is dispersive.

To address this problem, we first consider the Gaussian disorder model (GDM),[22] in which site energies, ϵ_i, are distributed according to the Gaussian density of states (GDOS), $p(\epsilon)=1/\sqrt{2\pi\sigma^2}\exp(-\epsilon^2/2\sigma^2)$. For a finite number of hopping sites, the carrier mean energy reads

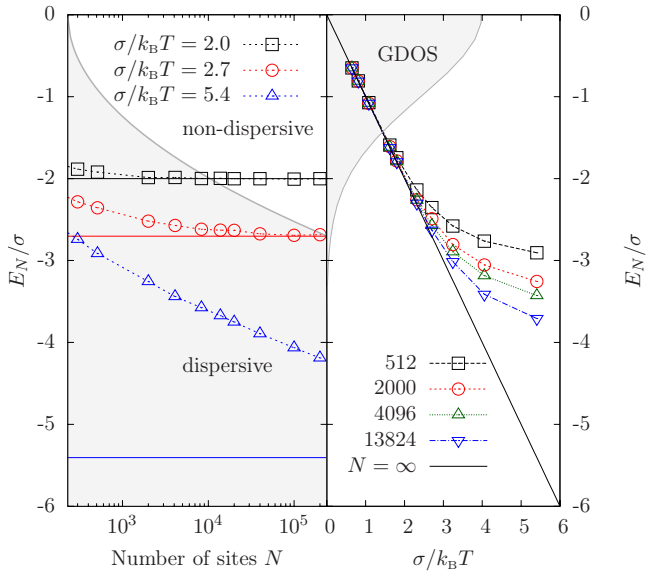

FIG. 1. (Color online) E_N (symbols) and E_∞ (solid lines) as a function of number of sites N (left) and inverse temperature (right). E_N is calculated by choosing N random numbers from the Gaussian distribution and evaluating the sum in Eq. (2). $\sigma/k_BT=5.4$ corresponds to 300 K for Alq_3, which has an energetic disorder of $\sigma=0.14$ eV. The gray area on the left plot (small N, large σ) defines the parameter space of the dispersive transport. GDOS is shown on the right plot.

$$E_N = \left\langle Z_N^{-1} \sum_{n=1}^{N} \epsilon_n e^{-\beta\epsilon_n} \right\rangle, \tag{2}$$

where $Z_N=\Sigma_{n=1}^{N} e^{-\beta\epsilon_n}$, $\langle\cdots\rangle$ denotes the average over all realizations of N-site energies, $\beta=1/k_BT$. In a system with an infinite number of sites, $N=\infty$, the mean energy is proportional to inverse temperature,[23,24] $E_\infty=-\partial_\beta \ln[\int_{-\infty}^{\infty} p(\epsilon)e^{-\beta\epsilon}d\epsilon]=-\sigma^2/k_BT$.

The dependencies of E_N/σ versus the number of sites, N, and the inverse temperature, σ/k_BT, are shown in Fig. 1. As expected, the carrier mean energies in finite-size systems are systematically higher than E_∞, i.e., mobility simulations in a small box would be performed at a higher temperature. Hence, one might expect that the mobility will decrease with the increase in system size.[25] A similar trend is observed for the temperature dependence of E_N/σ, where mean energies are higher than E_∞ for small temperatures and large values of energetic disorder. Analysis of these dependencies yields an empirical expression for the transition between the dispersive and nondispersive transport, for large N,[21]

$$(\sigma/k_BT)^2 = -5.7 + 1.05 \ln N. \tag{3}$$

For $\sigma/k_BT=2.7$, the asymptotic value E_∞ is achieved for $N>10^5$. For $\sigma/k_BT=5.4$, E_N is well above E_∞, even for $N>10^5$, i.e., significantly bigger systems are required to equilibrate a charge carrier in the GDOS with $\sigma=0.14$ eV at 300 K, which is a typical value of the energetic disorder of tris(8-hydroxyquinoline) aluminum (Alq_3) [see $N=294$,[15] $N=1137$,[13] and $N=320$ (Ref. 26)]. Moreover, Eq. (3) predicts that a brute-force increase in the number of sites, N, cannot resolve the problem for compounds with large energetic disorder since N increases exponentially with σ^2.

Equation (3) also hints at a possible solution. Indeed, the relevant dimensionless parameter is the half width of GDOS divided by temperature, σ/k_BT. Hence, the transition between dispersive and nondispersive transport can be shifted to lower values of N by simply increasing the temperature. At some elevated temperature, transport will eventually become nondispersive even for small box sizes. Provided the temperature dependence of the nondispersive mobility is known, its value can then be extrapolated to experimentally relevant temperatures.

Two prerequisites are needed to perform such an extrapolation. First, the simulation temperatures should be high enough for transport to be nondispersive for a given size of the simulation box. To do this, the transition temperature, T_{ND}, can be estimated via Eq. (3) from the value of energetic disorder σ (which can be obtained from the site energy distribution even in small systems) and the number of hopping sites, N. Nondispersive mobilities can then be calculated for a set of temperatures above T_{ND}. Second, an explicit temperature dependence of charge-carrier mobility is needed. In one dimension, the exact analytical expression for mobility is known for an arbitrary set of rates.[27–29] In the case of Marcus rates, the temperature dependence of the nondispersive mobility at zero field reads[29]

$$\mu(T) = \frac{\mu_0}{T^{3/2}} \exp\left[-\left(\frac{a}{T}\right)^2 - \left(\frac{b}{T}\right) \right], \tag{4}$$

where a, b, and μ_0 are material constants. Strictly speaking, this temperature dependence is valid in one dimension only. As we will see, it can still be used in a three-dimensional case in a very broad temperature range. A fit to Eq. (4) allows for the parameters μ_0, a, and b to be extracted. Finally,

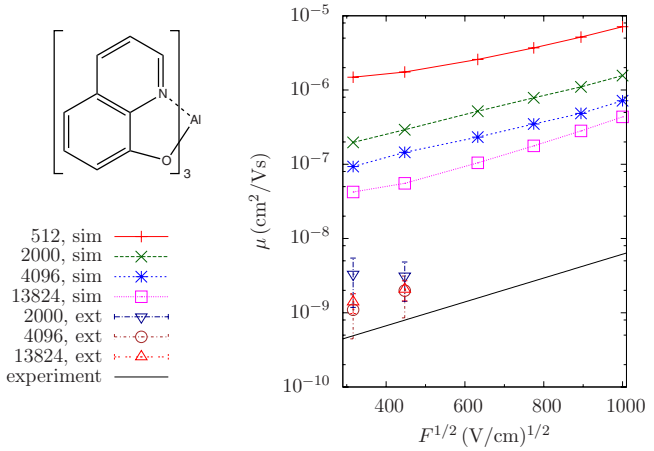

FIG. 2. (Color online) Chemical structure of Alq_3, simulated (sim) and extrapolated (ext) Alq_3 hole mobilities as a function of electric field for a set of box sizes (number of hopping sites, N). Strong variation in simulated mobilities with system size is typical for dispersive transport. Simulated values collapse on a single curve (in a zero-field limit) after extrapolation. Experimental mobilities are taken from Ref. 31. Poole-Frenkel behavior of the mobility (Refs. 31–33) $\mu=\mu_0 \exp(\gamma\sqrt{F})$, is also reproduced.

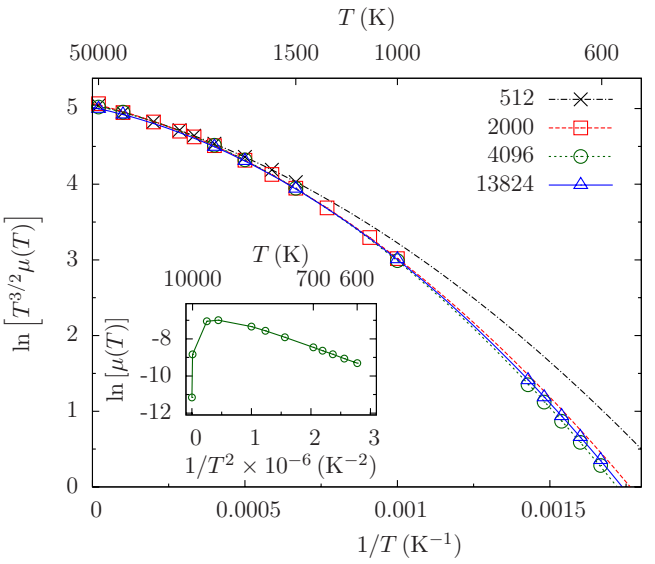

FIG. 3. (Color online) Temperature dependence of nondispersive hole mobility. $F=10^5$ V/cm. Points correspond to the simulation results, lines to fittings to Eq. (4). Inset shows that widely used GDM temperature dependence (Refs. 21 and 22), $\mu(T)=\mu_0 \exp[-(T_0/T)^2]$, can only be used in a limited temperature range, failing at high temperatures (Ref. 27).

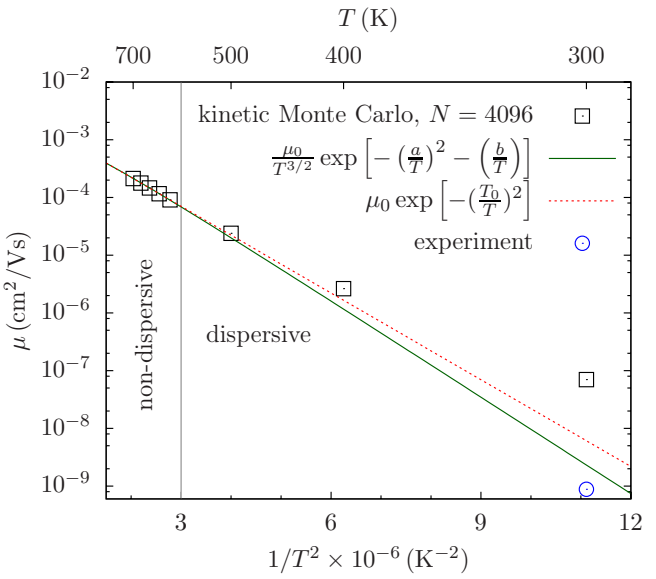

FIG. 4. (Color online) Alq_3 hole mobility as a function of temperature. $F=10^5$ V/cm. In the dispersive regime, mobility deviates from Eq. (4) as well as from a GDM-based low-field limit temperature dependence of charge-carrier mobility. As long as high temperatures are not required (for fitting), the difference between the GDM based and Eq. (4) functional forms is small.

the same expression is used to obtain the mobility at a desired temperature.[30]

To illustrate and test the extraction of nondispersive mobilities, we consider hole transport in amorphous films of tris(8-hydroxyquinoline) aluminum, a commonly used material in small-molecule organic light emitting diodes. Hole mobilities in amorphous Alq_3 are known to be nondispersive for a micrometer range thickness.[31–33]

The Poole-Frenkel plot, namely, room-temperature mobility as a function of the square root of an applied electric field, is shown in Fig. 2 for simulation boxes of 512, 2000, 4096, and 13 824 molecules.[34] The mobility is clearly system-size dependent and is several orders of magnitude larger than the experimentally reported value. After estimating T_{ND} for each N (for example, $T_{ND}(N=4096)\approx 600$ K), the mobility was calculated for a broad temperature range from 700 to 50 000 K for $T>T_{ND}(N)$. Simulation results together with the fit to Eq. (4) are shown in Fig. 3. The agreement is excellent and validates the ansatz used for the temperature dependence. A small deviation exists only for $N=512$, which is due to the limited accuracy of the fit since there are only a few points available above $T_{ND}(N=512)$. One should note that this is an additional limitation in the case of too small system sizes.

The results of the extrapolation are illustrated in Fig. 4, where both simulated and extrapolated mobilities are shown. At low temperatures, when transport is dispersive, simulated mobility is systematically higher than the value prescribed by Eq. (4). In this region, carrier mobility is system-size dependent. Above T_{ND}, mobility does not depend on the system size and its temperature dependence agrees well with Eq. (4). Finally, we calculated the nondispersive mobility at 290 K for two low values of the electric field, $F=10^5$ V/cm and 2×10^5 V/cm. The results are shown in Fig. 2 together with the TOF results obtained at 290 K.[31] One can see that both absolute values as well as the Poole-Frenkel behavior are very well reproduced. Given systematic errors of transfer integrals and site energies and the fact that TOF experiments provide slightly different mobilities depending on the coating rate for the amorphous film preparation,[31–33] the agreement between simulated and experimental values is excellent.

To summarize, we proposed an approach which can be used to obtain nondispersive charge-carrier mobilities from simulations in small systems, which provides a way to bridge length scales with different carrier dynamics.

This work was supported by DFG via IRTG program 1404, Grant No. AN 680/1-1 and SPP1355, MMM Initiative of the Max Planck Society, and the EuroSim EST program of Marie Curie actions. We thank M. Jochum, V. Rühle, F. May, and K. Johnston for critical reading of the manuscript.

*lukyanov@mpip-mainz.mpg.de
†denis.andrienko@mpip-mainz.mpg.de

[1] X. Feng, V. Marcon, W. Pisula, M. Hansen, J. Kirkpatrick, F. Grozema, D. Andrienko, K. Kremer, and K. Müllen, Nature Mater. **8**, 421 (2009).
[2] J.-L. Brédas, J. E. Norton, J. Cornil, and V. Coropceanu, Acc. Chem. Res. **42**, 1691 (2009).
[3] A. Troisi, D. L. Cheung, and D. Andrienko, Phys. Rev. Lett. **102**, 116602 (2009).
[4] V. Coropceanu, J. Cornil, D. A. da Silva Filho, Y. Olivier, R. Silbey, and J.-L. Bredas, Chem. Rev. **107**, 926 (2007).
[5] J. Kirkpatrick, V. Marcon, J. Nelson, K. Kremer, and D. Andrienko, Phys. Rev. Lett. **98**, 227402 (2007).
[6] T. Vehoff, B. Baumeier, A. Troisi, and D. Andrienko, J. Am. Chem. Soc. **132**, 11702 (2010).
[7] P. A. Lee and T. V. Ramakrishnan, Rev. Mod. Phys. **57**, 287 (1985).
[8] *Charge Transport in Disordered Solids*, edited by S. Baranovski (Wiley, Chichester, 2006).
[9] P. F. Barbara, T. J. Meyer, and M. A. Ratner, J. Phys. Chem. **100**, 13148 (1996).
[10] V. Marcon, W. Pisula, J. Dahl, D. W. Breiby, J. Kirkpatrick, S. Patwardhan, F. Grozema, and D. Andrienko, J. Am. Chem. Soc. **131**, 11426 (2009).
[11] Y. Olivier, L. Muccioli, V. Lemaur, Y. H. Geerts, C. Zannoni, and J. Cornil, J. Phys. Chem. B **113**, 14102 (2009).
[12] E. Di Donato, R. P. Fornari, S. Di Motta, Y. Li, Z. Wang, and F. Negri, J. Phys. Chem. B **114**, 5327 (2010).
[13] J. J. Kwiatkowski, J. Nelson, H. Li, J.-L. Bredas, W. Wenzel, and C. Lennartz, Phys. Chem. Chem. Phys. **10**, 1852 (2008).
[14] J. Nelson, J. Kwiatkowski, J. Kirkpatrick, and J. Frost, Acc. Chem. Res. **42**, 1768 (2009).
[15] Y. Nagata and C. Lennartz, J. Chem. Phys. **129**, 034709 (2008).
[16] V. Rühle, J. Kirkpatrick, and D. Andrienko, J. Chem. Phys. **132**, 134103 (2010).
[17] N. Vukmirović and L.-W. Wang, Phys. Rev. B **81**, 035210 (2010).
[18] B. Baumeier, J. Kirkpatrick, and D. Andrienko, Phys. Chem. Chem. Phys. **12**, 11103 (2010).
[19] Semiempirical methods, such as ZINDO, are more efficient since they require only precomputed monomer orbitals (Ref. 35). These methods are, however, not applicable for a large class of, e.g., metal-coordinated, compounds.
[20] H. Scher and E. W. Montroll, Phys. Rev. B **12**, 2455 (1975).
[21] P. Borsenberger, E. Magin, M. van der Auweraer, and F. de Schryver, Phys. Status Solidi A **140**, 9 (1993).
[22] P. M. Borsenberger, L. Pautmeier, and H. Bässler, J. Chem. Phys. **94**, 5447 (1991).
[23] M. Grünewald, B. Pohlmann, B. Movaghar, and D. Würtz, Philos. Mag. B **49**, 341 (1984).
[24] B. Movaghar, M. Grünewald, B. Ries, H. Bässler, and D. Würtz, Phys. Rev. B **33**, 5545 (1986).
[25] In experiments, temporal relaxation is normally discussed (Refs. 23 and 24), where mean energy is a function of time and $E(t \to \infty) = E_\infty$. While this approach is suitable for the interpretation of experimental data and time-of-flight-type simulations, where charges are injected on one and collected on the other side of the sample, in simulations with periodic boundary conditions it is more appropriate to consider mean carrier energy as a function of the total number of hopping sites N.
[26] N. G. Martinelli, M. Savini, L. Muccioli, Y. Olivier, F. Castet, C. Zannoni, D. Beljonne, and J. Cornil, Adv. Funct. Mater. **19**, 3254 (2009).
[27] H. Cordes, S. D. Baranovskii, K. Kohary, P. Thomas, S. Yamasaki, F. Hensel, and J. H. Wendorff, Phys. Rev. B **63**, 094201 (2001).
[28] B. Derrida, J. Stat. Phys. **31**, 433 (1983).
[29] K. Seki and M. Tachiya, Phys. Rev. B **65**, 014305 (2001).
[30] Since we are not interested in the actual temperature dependence of mobility but in its nondispersive value at a given temperature, the morphology equilibrated at this temperature is kept fixed. To study temperature dependence, e.g., an effect of a glass transition (Ref. 21), the procedure should be repeated for several, equilibrated at different temperatures, morphologies.
[31] H. Fong and S. So, J. Appl. Phys. **100**, 094502 (2006).
[32] W. Brütting, S. Berleb, and A. G. Mückl, Org. Electron. **2**, 1 (2001).
[33] S. Naka, H. Okada, Y. Onnagawa, T. Yamaguchi, and T. Tsutsui, Synth. Met. **111-112**, 331 (2000).
[34] Morphologies are obtained using molecular dynamics and modified OPLS force field (Ref. 36). To calculate the rates, the hole reorganization energy $\lambda = 0.23$ eV is used (Ref. 36). Transfer integrals are calculated using the intermediate neglect of differential overlap level of theory (ZINDO) (Ref. 35). The free-energy difference has an electrostatic and an external field contributions, $\Delta G_{ij} = e\boldsymbol{F} \cdot \boldsymbol{r}_{ij} + \Delta G_{\mathrm{el}}$. The electrostatic contribution, $\Delta G_{\mathrm{el}} = \epsilon_i - \epsilon_j$, is calculated using partial charges for charged and neutral Alq_3 molecules in the ground state obtained from density-functional-theory calculations [B3LYP/6-311g(d)] (Ref. 37). Polarization is treated phenomenologically by using distance-dependent dielectric constant (Ref. 15). Resulting site energies, ϵ_i, are approximately Gaussian distributed with a standard deviation of $\sigma = 0.14$ eV. Transfer rates, ω_{ij}, and molecular positions are used in KMC simulations with periodic boundary conditions. Charge carrier mobility is determined as $\mu = v/F$, where v is the averaged projection of the carrier velocity on the direction of the field F. Carrier mobilities are averaged over 100 MD snapshots and six different spatial directions. Simulations were performed using the VOTCA package (Ref. 38).
[35] J. Kirkpatrick, Int. J. Quantum Chem. **108**, 51 (2008).
[36] A. Lukyanov, C. Lennartz, and D. Andrienko, Phys. Status Solidi A **206**, 2737 (2009).
[37] J. Kirkpatrick, V. Marcon, K. Kremer, J. Nelson, and D. Andrienko, J. Chem. Phys. **129**, 094506 (2008).
[38] V. Rühle, C. Junghans, A. Lukyanov, K. Kremer, and D. Andrienko, J. Chem. Theory Comput. **5**, 3211 (2009).